

Reprinted from

---

# COMPUTATIONAL MATERIALS SCIENCE

---

Computational Materials Science 13 (1998) 132–141

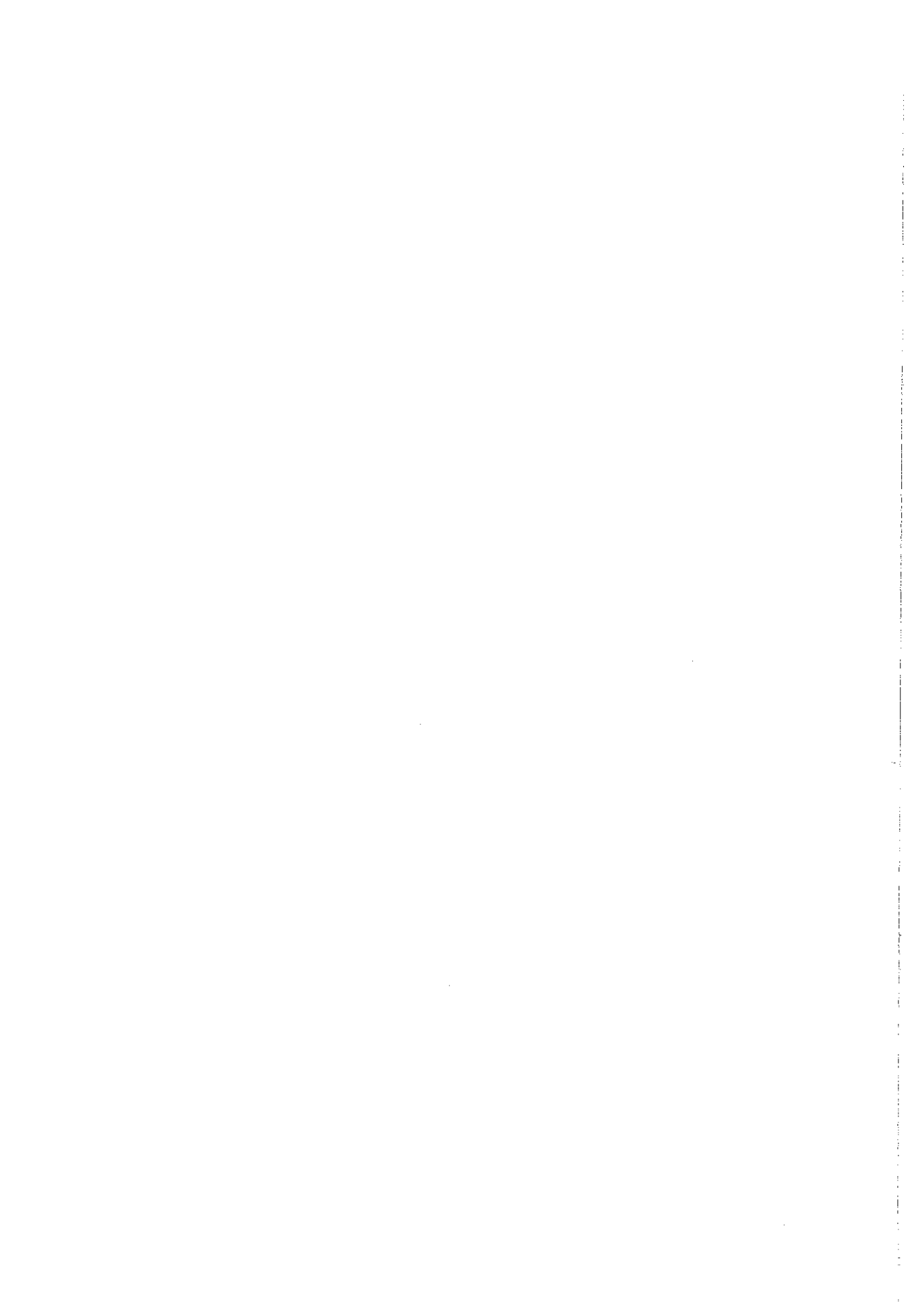
## Damage modeling of the single crystal superalloy SRR99 under monotonous creep

Weidong Qi <sup>a,\*</sup>, Albrecht Bertram <sup>b</sup>

<sup>a</sup> *Institute for Materials Research, GKSS Research Centre, Max-Planck-Strasse, D-21502 Geesthacht, Germany*

<sup>b</sup> *Institut für Mechanik, Otto-van-Guericke-Universität, D-39016 Magdeburg, Germany*





imperfections such as casting pores. Thus, the damage develops anisotropically. Therefore there is a need to develop constitutive models for the growth of creep strain and damage of single crystal superalloys by considering the influence of material and damage induced anisotropy. These models should on the one hand adequately represent material behavior, but, on the other, be as simple as possible so that they are in a form suitable for implementation into numerical codes such as FEM.

Advanced engineering materials subjected to extreme thermo-mechanical and environmental conditions undergo microstructural changes which reduce their deformation resistance. Bertram and Olschewski [5] proposed an anisotropic constitutive model for the description of the creep behavior of single crystals at high temperatures. This model has been applied to the creep behavior simulation of the single crystal superalloy SRR99 [6] and of CMSX-6 [7] at 760°C. However, the progressive degradation of the mechanical properties of such materials caused by irreversible microstructural changes during the creep process has not been considered in this approach. It is therefore restricted to the undamaged material behavior of the primary and secondary creep phase. In order to model the tertiary creep behavior and to predict the time to rupture, additional models are needed.

Continuum Damage Mechanics (CDM) as developed by Kachanov [8,9], Rabotnov [10], Hult [11], Krajcinovic and Lemaitre [12], Chaboche [13], Lemaitre [14] and others is a continuum mechanics approach to the deformation and rupture analysis. CDM concepts are supported by the general framework of thermodynamics of irreversible processes, and offer complementary possibilities to fracture mechanics [13]. In this paper, we will first briefly introduce the creep model for single crystal superalloys proposed by Bertram and Olschewski [5–7]. The focus will be on a phenomenological damage model developed on the grounds of the CDM theory by considering both the initial anisotropy of the material and the damage induced anisotropy, and on its application to the single crystal SRR99 at 760°C by using the effective stress concept of CDM. As such materials

have limited ductility, we apply only small deformation analysis. For simplicity, isothermal conditions are assumed so that the effect of temperature changes enters the constitutive equations only through the temperature dependence of the material parameters.

## 2. Creep model for single crystals

Starting from a uniaxial rheological four-parameter Burgers-model which consists of two springs and two dampers, Bertram and Olschewski [5] used a projection method to construct an anisotropic three-dimensional model for the description of the creep behavior of cubic single crystals at high temperatures. These constitutive equations can be written as:

$$\dot{\boldsymbol{\varepsilon}} = \mathbf{A}_1^{(4)} : \dot{\boldsymbol{\sigma}} + \mathbf{A}_2^{(4)} : \boldsymbol{\sigma} + \mathbf{A}_3^{(4)} : \boldsymbol{\tau}, \quad (1)$$

$$\dot{\boldsymbol{\tau}} = \mathbf{A}_4^{(4)} : \dot{\boldsymbol{\sigma}} + \mathbf{A}_5^{(4)} : (\boldsymbol{\sigma} - \boldsymbol{\tau}), \quad (2)$$

where  $\boldsymbol{\varepsilon}$  and  $\boldsymbol{\sigma}$  are the strain and stress tensor, respectively, and  $\boldsymbol{\tau}$  is an internal variable which corresponds, in uniaxial cases, to the stress in a spring. Herein

$$\mathbf{A}_1^{(4)} = \sum_{i=1}^3 \frac{1}{C_i + K_i} \mathbf{P}_i^{(4)}, \quad (3a)$$

$$\mathbf{A}_2^{(4)} = \sum_{i=1}^3 \frac{1}{C_i + K_i} \left( \frac{C_i}{D_i} + \frac{C_i}{L_i} + \frac{K_i}{L_i} \right) \mathbf{P}_i^{(4)}, \quad (3b)$$

$$\mathbf{A}_3^{(4)} = \sum_{i=1}^3 \frac{C_i}{C_i + K_i} \frac{1}{D_i} \mathbf{P}_i^{(4)}, \quad (3c)$$

$$\mathbf{A}_4^{(4)} = \sum_{i=1}^3 \frac{K_i}{C_i + K_i} \mathbf{P}_i^{(4)}, \quad (3d)$$

$$\mathbf{A}_5^{(4)} = \sum_{i=1}^3 \frac{K_i}{C_i + K_i} \frac{C_i}{D_i} \mathbf{P}_i^{(4)} \quad (3e)$$

are fourth-rank material tensors being linear combinations of three structure tensors

$$\mathbf{P}_1 = \frac{1}{3} \mathbf{I} \otimes \mathbf{I}, \quad (4a)$$

$$\mathbf{P}_2 = \mathbf{R} - \mathbf{P}_1, \quad (4b)$$

$$\mathbf{P}_3 = \mathbf{I} - \mathbf{P}_1 - \mathbf{P}_2, \quad (4c)$$

with

$$\mathbf{R} = \sum_{i=1}^3 \mathbf{e}_i^k \otimes \mathbf{e}_i^k \otimes \mathbf{e}_i^k \otimes \mathbf{e}_i^k, \quad (5)$$

where  $\mathbf{I}$  and  $\mathbf{I}^{(4)}$  denote the identity tensor of rank two and four, respectively,  $\otimes$  the tensor product,  $C_i, K_i, D_i, L_i$  ( $i = 1, 2, 3$ ) temperature-dependent material parameters, and  $\mathbf{e}_j^k$  ( $j = 1, 2, 3$ ) the lattice vectors. The dependence of the viscosities  $D_i$  and  $L_i$  on the applied stress is expressed as:

$$D_i = D_{0i} \exp \left\{ - \sum_j Z_{ij} J_j \right\}, \quad (6a)$$

$$L_i = L_{0i} \exp \left\{ - \sum_j Z_{ij} J_j \right\}, \quad (6b)$$

with material parameters  $Z_{ij}$  ( $i = 1, 2, 3, 4; j = 1, 2, 3$ ) and the following scalar invariants showing cubic symmetry

$$J_1 = \sqrt{\sigma_{11}\sigma_{22} + \sigma_{22}\sigma_{33} + \sigma_{33}\sigma_{11}}, \quad (7a)$$

$$J_2 = \sigma_{12}^2 + \sigma_{23}^2 + \sigma_{31}^2, \quad (7b)$$

$$J_3 = \sigma_{11}\sigma_{22}\sigma_{33}, \quad (7c)$$

$$J_4 = \sigma_{11}(\sigma_{12}^2 + \sigma_{13}^2) + \sigma_{22}(\sigma_{23}^2 + \sigma_{21}^2) + \sigma_{33}(\sigma_{31}^2 + \sigma_{32}^2). \quad (7d)$$

By the assumption that volume changes occur only elastically, it follows:

$$D_1^{-1} = 0, L_1^{-1} = 0 \quad \text{and} \quad Z_{i1} = 0 \quad (i = 1, 2, 3, 4). \quad (8)$$

In the limiting cases,  $D_i = \infty$  and  $L_i = \infty$  ( $i = 1, 2, 3$ ), the Eqs. (1) and (2) degenerate to Hooke's law.

### 3. The effective stress concept of CDM

Damage resulting from the development of microcracks and microvoids leads to creep acceleration in the tertiary creep phase. This effect can be described by adding the damage variables into the creep equation. As the degradation of the material structure caused by material damage implies an internal decrease of the load carrying area, Rabotnov [10] first introduced the notion of effective stress

$$\tilde{\sigma} = \frac{\sigma}{1-D}, \quad (9)$$

where  $\sigma$  is the stress and  $D$  is the damage variable, and modified Norton's steady stage creep law

$$\dot{\varepsilon}^c = A\sigma^w \quad (10)$$

by replacing the stress  $\sigma$  by the effective stress  $\tilde{\sigma}$ , i.e.

$$\dot{\varepsilon}^c = A\tilde{\sigma}^w = A \left( \frac{\sigma}{1-D} \right)^w, \quad (11)$$

where  $\varepsilon^c$  is the creep strain, and  $A$  and  $w$  are material parameters. The following evolution law of damage is then assumed to complete the model:

$$\dot{D} = G \left( \frac{\sigma}{1-D} \right)^r. \quad (12)$$

Two material parameters  $G$  and  $r$  are to be determined from creep tests. This model can describe fairly accurately the tertiary creep as well as the creep ductility in many materials in the one-dimensional case [15].

Following this idea it can be assumed that there exists a fictitious effective stress acting on the undamaged material that causes the same strains as the real stress acting on the damaged material. The effective stress concept has been expressed by Lemaitre [14]: "Any strain constitutive equation for a damaged material may be derived in the same way as for a virgin material except that the usual stress is replaced by the effective stress".

### 4. Phenomenological damage model

Microscopic investigations [16–18] show that the deterioration of nickel-based single crystal superalloys under creep loading conditions is directly

caused by the growth and coalescence of initial microcracks starting from casting pores. Material damage can be defined as a collection of permanent microstructural changes concerning the material thermomechanical properties (e.g. stiffness, strength, anisotropy, etc.) brought about in a material by irreversible physical microcracking processes resulting from the application of thermomechanical loading [19,20]. According to the principles of irreversible thermodynamics it is necessary to introduce internal variables, called damage variables, for the phenomenological description of material damage. Because of its microscopic nature damage has, in general, an anisotropic character even if the material is originally isotropic [21]. Therefore, tensor valued variables must be used for the three-dimensional representation of material damage [22]. In order to represent the state of anisotropic damage characterized by these cracks, we will employ a second rank symmetric damage tensor  $\mathbf{D}$  as a damage variable.

According to the effective stress concept, the classical continuum mechanics model for the undamaged material, such as the one described in Part 2, can be modified to include the damage influence. To accomplish this, a suitable definition of effective stress, which will replace the stress tensor in Eqs. (1) and (2), and a damage evolution law are needed.

#### 4.1. Effective stress and damage deactivation

Let a fourth-order tensor  $\overset{(4)}{\mathbf{M}}(\mathbf{D})$  characterize the damage state. The following general form of the transformation between the stress tensor  $\boldsymbol{\sigma}$  and the effective stress tensor  $\tilde{\boldsymbol{\sigma}}$  is assumed [15,23]:

$$\tilde{\boldsymbol{\sigma}} = \overset{(4)}{\mathbf{M}}(\mathbf{D}) : \boldsymbol{\sigma}. \quad (13)$$

Following the suggestion of Cordebois and Sidoroff [24], the previous transformation is taken in the particular form

$$\overset{(4)}{\mathbf{M}} = (\mathbf{I} - \mathbf{D})^{-1/2} \wedge (\mathbf{I} - \mathbf{D})^{-1/2}, \quad (14)$$

where the composition of two second-order tensors denoted by the wedge  $\wedge$  is defined as

$\mathbf{A} \wedge \mathbf{B} = a_{ij}b_{kl}(\mathbf{e}_i \otimes \mathbf{e}_k \otimes \mathbf{e}_j \otimes \mathbf{e}_l)$  for an orthonormal basis  $\mathbf{e}_i$ . This suggestion for  $\overset{(4)}{\mathbf{M}}(\mathbf{D})$  is identical to the one of Chow and Wang [25,26], and has been applied to the dynamic fracture of brittle anisotropic solids [27] and to the analytical prediction of the initiation and propagation of ductile fracture in metals [28]. However, it does not consider the deactivation of damage due to crack closure.

In order to illustrate the assumed damage process, we consider a single crack embedded in an elastic material with a tensile load perpendicular to the crack. If the load is reversed, the crack will close and in a one-dimensional case the material behaves as uncracked. This phenomenon is called damage deactivation (not healing) in CDM. The damage still exists but the loading condition can render it inactive. For the representation of this mechanism the phenomenological algorithm proposed by Hansen and Schreyer [29] is used in the present model. In this method the microcrack opening/closing effect is described by considering the spectral decomposition of the elastic strain tensor  $\boldsymbol{\varepsilon}^e$  and the total strain tensor  $\boldsymbol{\varepsilon}$

$$\boldsymbol{\varepsilon}^e = \sum_{i=1}^3 \varepsilon_i^e \mathbf{n}_{ei}^e \otimes \mathbf{n}_{ei}^e, \quad (15a)$$

$$\boldsymbol{\varepsilon} = \sum_{i=1}^3 \varepsilon_i \mathbf{n}_i^e \otimes \mathbf{n}_i^e, \quad (15b)$$

where  $\varepsilon_i^e$  and  $\varepsilon_i$  are the  $i$ th eigenvalues,  $\mathbf{n}_{ei}^e$  and  $\mathbf{n}_i^e$  are the corresponding  $i$ th eigenvectors of  $\boldsymbol{\varepsilon}^e$  and  $\boldsymbol{\varepsilon}$ , respectively. The positive (tensile) spectral tensor corresponding to the elastic and to the total strain are defined as

$$\mathbf{H}_{ee} = \sum_{i=1}^3 h(\varepsilon_i^e) \mathbf{n}_{ei}^e \otimes \mathbf{n}_{ei}^e, \quad (16a)$$

$$\mathbf{H}_e = \sum_{i=1}^3 h(\varepsilon_i) \mathbf{n}_i^e \otimes \mathbf{n}_i^e, \quad (16b)$$

respectively, where  $h(x)$  is the Heaviside function

$$h(x) = \begin{cases} 0 & \text{for } x \leq 0, \\ 1 & \text{for } x > 0, \end{cases} \quad (17a)$$

or, if one wants to avoid the discontinuity of stress-strain response, the following smooth function proposed in [29] can be used:

$$h(x) = \begin{cases} 0 & \text{for } x \leq x_m, \\ \frac{1}{2} \left\{ 1 - \cos \left[ \frac{\pi(x-x_m)}{x_p-x_m} \right] \right\} & \text{for } x_m < x < x_p, \\ 1 & \text{for } x \geq x_p, \end{cases} \quad (17b)$$

where  $x_m$  and  $x_p$  are two additional parameters. The positive spectral projection operators (fourth-order tensor) for the elastic and the total strains are defined as

$$\mathbf{P}_{ee}^{(4)} = \mathbf{H}_{ee} \wedge \mathbf{H}_{ee}, \quad (18a)$$

$$\mathbf{P}_e^{(4)} = \mathbf{H}_e \wedge \mathbf{H}_e, \quad (18b)$$

respectively. The positive projection of the elastic and the total strain tensors are then given by

$$\boldsymbol{\varepsilon}^{e+} = \mathbf{P}_{ee}^{(4)} : \boldsymbol{\varepsilon}^e, \quad (19a)$$

$$\boldsymbol{\varepsilon}^+ = \mathbf{P}_e^{(4)} : \boldsymbol{\varepsilon}, \quad (19b)$$

respectively, where the symbol  $:$  denotes the double contraction. By introducing a strain-based positive projection operator

$$\mathbf{T}^{(4)} = \mathbf{I}^{(4)} - \left( \mathbf{I}^{(4)} - \mathbf{P}_{ee}^{(4)} \right) : \left( \mathbf{I}^{(4)} - \mathbf{P}_e^{(4)} \right) \quad (20)$$

the active damage tensor is then given by

$$\mathbf{D}_a = \mathbf{T}^{(4)} : \mathbf{D}. \quad (21)$$

Thus, the effective stress tensor with respect to damage deactivation is defined as

$$\tilde{\boldsymbol{\sigma}} = (1 - \mathbf{D}_a)^{-1/2} \cdot \boldsymbol{\sigma} \cdot (1 - \mathbf{D}_a)^{-1/2}. \quad (22)$$

#### 4.2. Damage evolution equation

By assuming a decoupling of intrinsic and thermal dissipation and, for practical purposes, by postulating that the dissipation due to the damage processes and the dissipation associated with the other mechanisms such as the plastic strain and the hardening process, are independent [30], the dual dissipation potential  $\phi$  can be written as

$$\phi = \phi_T + \phi_M + \phi_D, \quad (23)$$

where  $\phi_T$ ,  $\phi_D$  and  $\phi_M$  are the dual potentials associated with thermal, damage, and other mechanisms, respectively. Since

$$\frac{\partial \phi_T}{\partial \mathbf{Y}_D} = 0, \quad (24a)$$

$$\frac{\partial \phi_M}{\partial \mathbf{Y}_D} = 0 \quad (24b)$$

the damage evolution law is given in [31,32]

$$\dot{\mathbf{D}} = \frac{\partial \phi}{\partial \mathbf{Y}_D} = \frac{\partial \phi_D}{\partial \mathbf{Y}_D}, \quad (24c)$$

where  $\mathbf{Y}_D$  is the thermodynamic force associated with damage, called *damage driving force*. To avoid complicated numerical computation, a quadratic form is chosen for the expression of the damage dissipation potential

$$\phi_D = \frac{1}{2} \mathbf{Y}_D : \mathbf{S}^{(4)} : \mathbf{Y}_D, \quad (25)$$

where the fourth-order structure tensor  $\mathbf{S}^{(4)}$  must be symmetric and positive-definite (thermodynamic restrictions). The damage evolution law is then given by

$$\dot{\mathbf{D}} = \mathbf{S}^{(4)} : \mathbf{Y}_D. \quad (26)$$

In order to simplify the problem, we consider at first isotropic materials. In this case, damage development in a creep process generally depends on the current state of stress and damage. The damage law can be expressed as

$$\dot{\mathbf{D}} = \mathbf{G}(\boldsymbol{\sigma}, \mathbf{D}). \quad (27)$$

Analogous to the effective stress, which represents the effect of stress and damage on the strain response, a *damage active stress*  $\hat{\boldsymbol{\sigma}}$  can be assumed to represent the contributions of both the stress and the damage state to the damage growth. As experimental observations show that the creep rate is less sensitive to the damage state in comparison with the rate of void growth [33], the damage active stress is defined as

$$\hat{\boldsymbol{\sigma}} = (1 - \mathbf{D}_a)^{-p} \cdot \boldsymbol{\sigma} \cdot (1 - \mathbf{D}_a)^{-p}, \quad (28)$$

with a material parameter  $p$  which is used to distinguish the effect of damage on the damage growth from that on the creep rate. Thus, the damage development can be assumed to be only dependent on the damage active stress. On the other hand, according to thermodynamics, the damage driving force is responsible for the damage development. Based on the results of the microscopic investigations we assume that only the tensile damage active stresses are responsible for the damage growth, and that for isotropic materials the anisotropy of damage development only depends on the principal directions of damage active stress tensor. Motivated by these considerations and the uniaxial damage model of Kachanov and Rabotnov, we postulate the following expression for the damage driving force for isotropic materials

$$Y_D = \langle \hat{\sigma} \rangle^n = \sum_{i=1}^3 \langle \hat{\sigma}_i \rangle^n \mathbf{n}_i^\sigma \otimes \mathbf{n}_i^\sigma, \quad (29)$$

where  $n$  is a material parameter,  $\hat{\sigma}_i$  and  $\hat{\mathbf{n}}_i^\sigma$  are the  $i$ th eigenvalue and eigenvector of  $\hat{\sigma}$ , and  $\langle \cdot \rangle$  is the McCauley bracket, which equals one for positive arguments and zero otherwise.

For an anisotropic material, however, the damage will develop differently if the same tensile stress acts in different directions. In order to obtain the creep potential of anisotropic solids, Betten [34] proposed to map the actual creep state of an anisotropic solid onto a fictitious isotropic state with equivalent creep rate by a suitable transformation. The anisotropic behavior is described by using a *mapped stress tensor* instead of the actual stress tensor in the isotropic creep potential. Following this idea, we introduce the *mapped damage active stress*  $\hat{\sigma}_m$  with the help of an orientation function  $\eta_i$

$$\hat{\sigma}_m = \sum_{i=1}^3 (\eta_i \hat{\sigma}_i) \hat{\mathbf{n}}_i^\sigma \otimes \hat{\mathbf{n}}_i^\sigma. \quad (30)$$

The orientation function  $\eta_i$  modifies the effect of the  $i$ th principal damage active stress  $\hat{\sigma}_i$  depending on its orientation related to the material structure. For single crystals with cubic symmetry we suggest the following orientation function:

$$\eta_i = \left[ \sum_{j=1}^3 (\hat{\mathbf{n}}_i^\sigma \cdot \mathbf{e}_j^k)^{2m} \right]^q \quad (31)$$

where  $m$  and  $q$  are material parameters, and  $\mathbf{e}_j^k$  ( $j = 1, 2, 3$ ) are the lattice vectors. The damage driving force (with respect to material symmetry) is then given by

$$Y_D = \sum_{i=1}^3 \langle \eta_i \hat{\sigma}_i \rangle^n \hat{\mathbf{n}}_i^\sigma \otimes \hat{\mathbf{n}}_i^\sigma. \quad (32)$$

For cubic single crystals, we consider the following expression of the structure tensor  $\mathbf{S}$  (see Eqs. (4a)–(4c))

$$\mathbf{S} = \xi_1 \mathbf{P}_1 + \xi_2 \mathbf{P}_2 + \xi_3 \mathbf{P}_3, \quad (33)$$

where  $\xi_1$ ,  $\xi_2$  and  $\xi_3$  are material parameters. From Eqs. (4a)–(4c) we obtain

$$\mathbf{S} = \beta_1 \mathbf{I} \otimes \mathbf{I} + \beta_2 \mathbf{I} + \beta_3 \mathbf{R}, \quad (34)$$

with

$$\beta_1 = \frac{\xi_1 - \xi_2}{3}, \quad \beta_2 = \xi_2, \quad \beta_3 = \xi_2 - \xi_3. \quad (35)$$

Substituting Eqs. (32) and (34) into Eq. (26), we obtain the damage evolution law

$$\dot{\mathbf{D}} = \left( \beta_1 \mathbf{I} \otimes \mathbf{I} + \beta_2 \mathbf{I} + \beta_3 \mathbf{R} \right) : \sum_{i=1}^3 \langle \eta_i \hat{\sigma}_i \rangle^n \hat{\mathbf{n}}_i^\sigma \otimes \hat{\mathbf{n}}_i^\sigma \quad (36)$$

or, alternatively

$$\dot{\mathbf{D}} = \left( \alpha_1 \mathbf{I} \otimes \mathbf{I} + \alpha_2 \mathbf{I} + \alpha_3 \mathbf{R} \right) : \sum_{i=1}^3 \left\langle \frac{\eta_i \hat{\sigma}_i}{B} \right\rangle^n \hat{\mathbf{n}}_i^\sigma \otimes \hat{\mathbf{n}}_i^\sigma, \quad (37)$$

with

$$\alpha_1 + \alpha_2 + \alpha_3 = 1. \quad (38)$$

### 4.3. Rupture criterion

Kachanov [8] assumed that the final rupture of the material in creep occurs when the scalar damage variable  $D$  is equal to unity. In fact, there are critical values of the scalar damage variable

corresponding to the rupture of the element [35,36]. Lemaitre suggested that for metals this value is less than one and varies from 0.2 to 0.8. For our three-dimensional model we assume that creep rupture occurs when the first principal value  $D_I$  of the damage tensor is equal to a critical value  $D_R$ . The resulting material parameters of the present damage model are  $\alpha_1, \alpha_2, (\alpha_3 = 1 - \alpha_1 - \alpha_2), B, n, p, m, q$  and  $D_R$ .

**5. Creep model coupled with material damage**

Replacing the stress in Eqs. (1), (2), (7a), (7b), (7c) and (7d) by the effective stress defined in Eq. (22), we obtain the anisotropic creep model coupled with material damage

$$\dot{\epsilon} = \mathbf{A}_1^{(4)} : \dot{\bar{\sigma}} + \mathbf{A}_2^{(4)} : \dot{\bar{\sigma}} + \mathbf{A}_3^{(4)} : \tau, \tag{39}$$

$$\dot{\tau} = \mathbf{A}_4^{(4)} : \dot{\bar{\sigma}} + \mathbf{A}_5^{(4)} : (\bar{\sigma} - \tau), \tag{40}$$

where the material tensors  $\mathbf{A}_i$  ( $i = 1, \dots, 4$ ) depend on the cubic invariants of the effective stresses analogous to Eqs. (3a)–(8). Note that a transformation from  $\tau$  to some  $\tilde{\tau}$  as for  $\sigma$  is not needed.

**6. Theoretical predictions and comparison with experimental results**

Bertram and Olschewski [6] have identified the material parameters of their creep model for the nickel-based superalloy SRR99 at 760°C. The corresponding material parameters of the damage model are adopted from the work of Qi and Bertram [37], and are shown in Table 1. It is easy to see from the damage evolution law (28) and (36) that only the parameters  $B, n$  and  $p$  will be active if an uniaxial load acts in the [0 0 1]-orientation. Therefore we recommend to identify the parame-

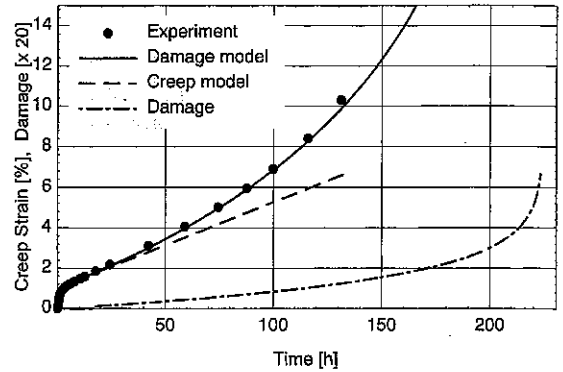


Fig. 1. Model prediction and experimental data of test MTU02 ( $\varphi_1 = 8^\circ, \varphi_2 = 8^\circ, \sigma = 800$  MPa).

ters  $B, n$  and  $p$  at first by calibrating the numerical values by uniaxial experiments with specimens of [0 0 1]-orientation. For the identification of material parameters, the optimization packages MINPACK and NAG Libraries have been used. The Heun-method has been applied for the numerical integration.

The creep tests were conducted at MTU and at BAM-V.21. Fig. 1 shows measured and simulated strains and the calculated damage of the creep test MTU02. The applied load is 800 MPa and the crystal orientation of the specimen is characterized by the Eulerian angles  $\varphi_1 = 8^\circ$  and  $\varphi_2 = 8^\circ$ , determining the orientation of the crystal relative to the load axis. Note that  $\varphi_2 = 0$  characterizes the ideal [0 0 1]-orientation. Creep model means the calculation by using Eqs. (1) and (2), and the *damage model* means the calculation by using Eqs. (39) and (40). *Damage* denotes the first principal value of the damage tensor  $\mathbf{D}$  multiplied by 20 (so that it appears in the same range as the creep curve). Figs. 2 and 3 give the comparison of the theoretical predictions and the experimental data as well as the damage development for two tests with different orientations, MTU06 ( $\varphi_1 = 45^\circ, \varphi_2 = 15^\circ$ ) and MTU21 ( $\varphi_1 = 40^\circ, \varphi_2 = 16^\circ$ ), which are performed under the same loading conditions as

Table 1  
Material parameters of damage model (SRR99 at 760°C)

$\alpha_1$	$\alpha_2$	$B$ (MPa)	$n$	$p$	$m$	$q$	$D_R$
0.0	0.5	1442.0	14.13	0.4549	51.85	-0.3133	0.2



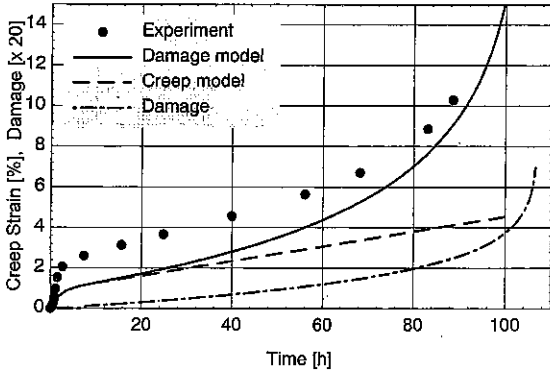


Fig. 2. Model prediction and experimental data of test MTU06 ( $\varphi_1 = 45^\circ$ ,  $\varphi_2 = 15^\circ$ ,  $\sigma = 800$  MPa).

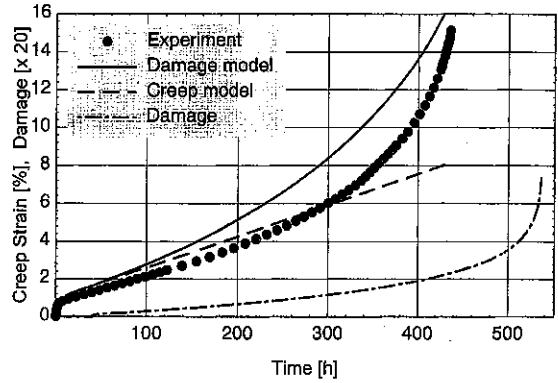


Fig. 4. Model prediction and experimental data of test BAM12 ( $\varphi_1 = 0^\circ$ ,  $\varphi_2 = 8.5^\circ$ ,  $\sigma = 750$  MPa).

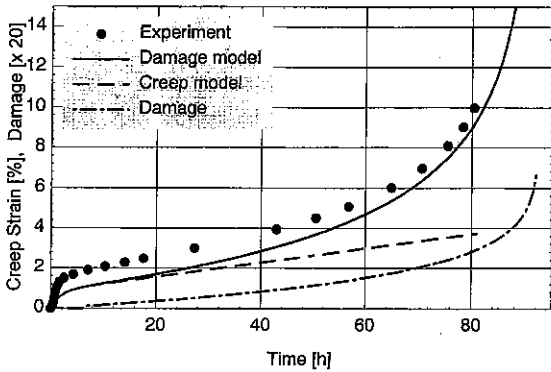


Fig. 3. Model prediction and experimental data of test MTU21 ( $\varphi_1 = 40^\circ$ ,  $\varphi_2 = 16^\circ$ ,  $\sigma = 800$  MPa).

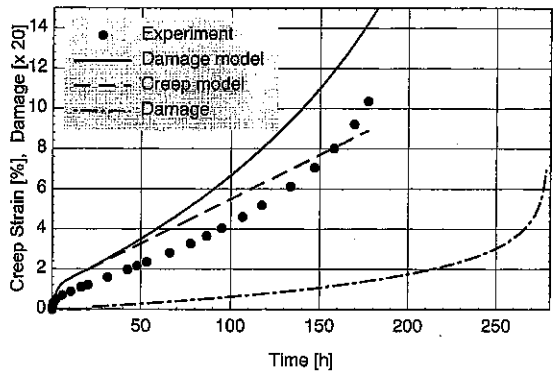


Fig. 5. Model prediction and experimental data of test MTU 20 ( $\varphi_1 = 0^\circ$ ,  $\varphi_2 = 4^\circ$ ,  $\sigma = 800$  MPa).

MTU02. Note the different time-scales of the diagrams. Figs. 1–3 show that the used damage model reflects the anisotropic damage development and its influence on the anisotropic creep behavior. The coupled model with damage simulates the complete creep behavior till rupture, and can thus be used for the prediction of life time.

The strong nonlinearity of the stress–strain response is shown in Figs. 4–6 for a fixed crystal orientation. The difference between the model and the experimental data lies within the scatter band inherent to such tests.

The damage variable starts to grow rather early, so that the second or steady creep phase exists only in an approximate sense. This corresponds to the

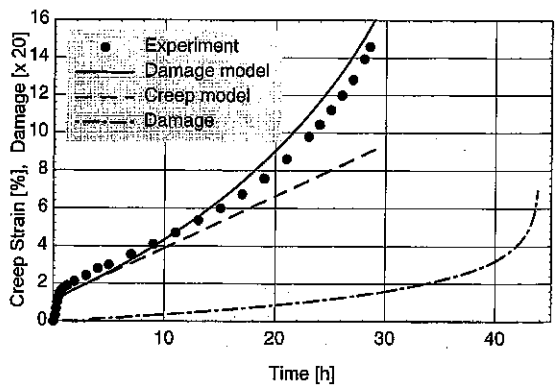


Fig. 6. Model prediction and experimental data of test BAM21 ( $\varphi_1 = 0^\circ$ ,  $\varphi_2 = 7.5^\circ$ ,  $\sigma = 900$  MPa).

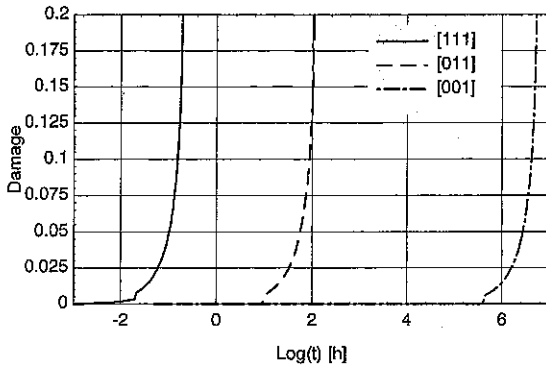


Fig. 7. Modeling of the damage development for the three extreme orientations ( $\sigma = 400$  MPa).

experimental finding that the overlinearity of the creep curve of superalloys begins right after the state of minimal creep rate. Fig. 7 shows the theoretical prediction of the damage development under constant load  $\sigma = 400$  MPa for the three extreme orientations.

## 7. Conclusion

A phenomenological model for the description of creep damage of single crystal superalloys is presented. Its application to the single crystal superalloy SRR99 demonstrates that the presented model provides satisfying prediction of the damage process and the life time in the range of the uniaxial monotonous creep. Both the influence of the material symmetry on the creep behavior and the nonlinearity of the material response with respect to the applied loads are reproduced by the present model. In order to test the capability of this model, especially for the case of multiaxial loading condition, further experimental investigations are needed. In this case, the choice of the relationship between the material parameters  $\alpha_1$ ,  $\alpha_2$  and  $\alpha_3$  plays an important role. As it is rather difficult and costly to conduct multiaxial experiments for single crystals, theoretical investigations on the development of damage under multidimensional loads and in particular on its dependence on nonproportional loads are of special interest.

## Acknowledgements

The authors would like to thank MTU (Munich) and BAM-V.21 (Berlin) for providing the test data for this work.

## References

- [1] S.X. Li, D.J. Smith, *Fatigue Fract. Engrg Mater. Struct.* 18 (1995) 617.
- [2] S.X. Li, D.J. Smith, *Fatigue Fract. Engrg Mater. Struct.* 18 (1995) 631.
- [3] R. Kunkel, *Untersuchungen zur Parameteridentifikation für das vereinheitlichte Modell nach Choi und Krempl am Beispiel der einkristallinen Nickel-Basislegierung SRR99*, Dissertation (TH Darmstadt), VDI Verlag, Düsseldorf, 1996.
- [4] R. Kunkel, F.G. Kollmann, *Acta Mechanica*. 124 (1997) 27.
- [5] A. Bertram, J. Olschewski, *ZAMM* 73 (1993) 4–5.
- [6] A. Bertram, J. Olschewski, *J. Comp. Mat. Sci.* 5 (1996) 12.
- [7] A. Bertram, J. Olschewski, *Math. Modelling and Sci. Comp.*, special issue (in press).
- [8] L.M. Kachanov, *IVZ Akad. Nauk. S.S.R. Otd. Tech. Nauk.* 8, 1958.
- [9] L.M. Kachanov, *Introduction to Continuum Damage Mechanics*, Kluwer Academic Publishers, Dordrecht, 1986.
- [10] Y.N. Rabotnov, in: M. Hetenyi, W.G. Vincenti (Eds.), *Proceedings of the 12th International Congress of Applied Mechanics*, Stanford 1968, Springer, Berlin, 1969, p. 342.
- [11] J. Hult, *Mechanisms of Deformation and Fracture*, Pergamon Press, Oxford, 1979, p. 233.
- [12] D. Krajcinovic, J. Lemaitre, *Continuum Damage Mechanics – Theory and Applications*, Springer, New York, 1987.
- [13] J.L. Chaboche, *J. Appl. Mech.* 55 (1988) 59.
- [14] J. Lemaitre, *A Course on Damage Mechanics*, Springer, Berlin, 1992.
- [15] J.L. Chaboche, *Nucl. Engrg. and Design* 79 (1984) 309.
- [16] S.H. Ai, V. Lupinc, in: E. Bachelet et al. (Eds.), *Proceedings of the High Temperature Materials for Power Engineering*, Liège, Belgium, 1990, Part II, p. 1027.
- [17] P.D. Portella, C. Herzog, 15 *Vortragsveranstaltung des DVM/DGM Arbeitskreises, Rasterelektronenmikroskopie in der Materialprüfung*, DVM, Berlin, 1992, p. 51.
- [18] M. Rumi, W. Chen, W. Wever, D. Mukherji, T. Kuttner, R.P. Wahi, in: D. Coutsouradis (Ed.), *Materials for Advanced Power Engineering, Part II*, 1994, p. 1165.
- [19] R. Talreja, *Proc. R. Soc. London Ser. A* 399 (1985) 195.
- [20] J.W. Ju, *Int. J. Solids and Structures* 25 (1989) 803.
- [21] J. Betten, *Journal de Mécanique Théorique et Appliquée* 2 (1983) 13.
- [22] F.A. Leckie, E.T. Onat, in: J. Hult, J. Lemaitre (Eds.), *Proceedings of the IUTAM Symposium on Physical Non-Linearities in Structural Analysis*, Springer, Berlin, 1981, p. 140.

- [23] J.L. Chaboche, Nucl. Engrg. and Design 64 (1981) 233.
- [24] J.P. Cordebois, F. Sidoroff, in: J.-P. Boehler (Ed.), Mechanical Behavior of Anisotropic Solids, Martinus Nijhoff, Boston, 1982, p. 761.
- [25] C.L. Chow, J. Wang, Engrg Frac. Mech. 27 (1987) 547.
- [26] C.L. Chow, J. Wang, Int. J. Fracture 33 (1987) 3.
- [27] E.P. Fahrenthold, in: J.W. Ju (Ed.), Damage Mechanics in Engineering Materials, 1990, p. 251.
- [28] J.S. Jubran, W.F. Cofer, Computers and Structures 39 (1991) 741.
- [29] N.H. Hansen, H.L. Schreyer, J. Appl. Mech. 62 (1995) 450.
- [30] T.J. Lu, C.L. Chow, J. Theory Appl. Fract. Mech. 14 (1990) 187.
- [31] P. Germain, Q.S. Nguyen, P. Suquet, J. Appl. Mech. 50 (1983) 1010.
- [32] D. Krajcinovic, J. Appl. Mech. 50 (1983) 355.
- [33] S. Murakami, N. Ohno, in: A.R.S. Ponter, D.R. Hayhurst (Eds.), Creep in Structures, Springer, Berlin, 1981, p. 422.
- [34] J. Betten, J. of Rheology 25 (1981) 565.
- [35] G. Piatti, G. Bernasconi, F.A. Cozarelli, Trans. 5th Int. Conf. SMiRT, Berlin 1979, North-Holland, Amsterdam, vol. L, L11/4, 1979.
- [36] A. Litewka, in: J.P. Boehler (Ed.), Yielding Damage and Failure of anisotropic Solids EGF5, 1990, p. 655.
- [37] W. Qi, A. Bertram, Technische Mechanik 17 (1997) 313.



# COMPUTATIONAL MATERIALS SCIENCE

## Instructions to Authors

### Submission of papers

Manuscripts (one original + two copies), accompanied by a covering letter, should be sent to one of the Editors indicated on page 2 of the cover.

**Original material.** By submitting a paper for publication in Computational Materials Science the authors imply that the material has not been published previously nor has been submitted for publication elsewhere and that authors have obtained the necessary authority for publication.

**Refereeing.** Submitted papers will be refereed and, if necessary, authors may be invited to revise their manuscript. If a submitted paper relies heavily on unpublished material, it would be helpful to have a copy of that material for the use of the referee.

### Types of contributions

Original research papers, reviews, letters to the editor and commentaries are welcome. They should contain an Abstract (of up to 200 words) and a Conclusions section which, particularly in the case of theoretical papers, translates the results into terms readily accessible to most readers.

### Manuscript preparation

All manuscripts should be written in good English. The paper copies of the text should be prepared with double line spacing and wide margins, on numbered sheets. See notes opposite on electronic versions of manuscripts.

**Structure.** Please adhere to the following order of presentation: Article title, Author(s), Affiliation(s), Abstract, PACS codes and keywords, Main text, Acknowledgements, Appendices, References, Figure captions, Tables.

**Corresponding author.** The name, complete postal address, telephone and fax numbers and the e-mail address of the corresponding author should be given on the first page of the manuscript.

**PACS codes/keywords.** Please supply one or more relevant PACS-1995 classification codes and 6-8 keywords of your own choice for indexing purposes.

**References.** References to other work should be consecutively numbered in the text using square brackets and listed by number in the Reference list.

### Illustrations

Illustrations should also be submitted in triplicate: one master set and two sets of copies. The *line drawings* in the master set should be original laser printer or plotter output or drawn in black india ink, with careful lettering, large enough (3-5 mm) to remain legible after reduction for printing. The *photographs* should be originals, with somewhat more contrast than is required in the printed version. They should be unmounted unless part of a composite figure. Any scale markers should be inserted on the photograph, not drawn below it.

**Colour plates.** Figures may be published in colour, if this is judged essential by the Editor. The Publisher and the author will each bear part of the extra costs involved. Further information is available from the Publisher.

### After acceptance

**Notification.** You will be notified by the Editor of the journal of the acceptance of your article and invited to supply an electronic version of the accepted text, if this is not already available.

**Copyright transfer.** You will be asked to transfer the copyright of the article to Publisher. This transfer will ensure the widest possible dissemination of information.

### Electronic manuscripts

The Publisher welcomes the receipt of an electronic version of your accepted manuscript (*enclosed in LaTeX*). If you have not already supplied the final, revised version of your article (on diskette) to the Journal Editor, you are requested herewith to send a file with the text of the accepted manuscript directly to the Publisher by e-mail or on diskette (allowed formats 3.5" or 5.25" MS-DOS, or 3.5" Macintosh) to the address given below. Please note that no deviations from the version accepted by the Editor of the journal are permissible without the prior and explicit approval by the Editor. Such changes should be clearly indicated on an accompanying printout of the file.

LaTeX articles should preferably use the Elsevier document class 'elsart', or alternatively the standard document class 'article' or the document style 'revtex'.

The Elsevier LaTeX package (including detailed instructions to authors) can be obtained using anonymous FTP from the Comprehensive TeX Archive Network (CTAN) from the directory: /texarchive/macros/latex/contrib/supported/elsevier.

The participating hosts in the Comprehensive TeX Archive Network are: ftp.dante.de (Germany), ftp.tex.ac.uk (UK).

For a WWW interface to CTAN with the possibility to search the archive, visit the URL 'http://www.ucc.ie/cgi-bin/ctan/'. For a list of hosts maintaining a (partial) mirror of the CTAN archive, see the file '/texarchive/CTAN.sites' on CTAN. In order to reduce network load, it is recommended that you use the CTAN host which is located in the closest network proximity to your site. Alternatively, you may wish to obtain a copy of the CTAN via CD-ROM (see 'help/CTAN.cdrrom' on CTAN for details).

Questions concerning the LaTeX author-prepared article project and requests for the booklet with instructions to authors should be directed to the address below.

If sent via electronic mail, files should be accompanied by a clear identification of the article (name of journal, editor's reference number) in the 'subject field' of the electronic-mail message. An ASCII table (available from the publisher) should be included in the files, to enable any transmission errors to be detected.

### Author benefits

**No page charges.** Publishing in Computational Materials Science is free.

**Free offprints.** The corresponding author will receive 50 offprints free of charge. An offprint order form will be supplied by the Publisher for ordering any additional paid offprints.

**Discount.** Contributors to Elsevier Science journals are entitled to a 30% discount on all Elsevier Science books.

**Contents Alert.** Papers scheduled for publication in Computational Materials Science are included in Elsevier's pre-publication service Contents Alert.

### Further information (after acceptance)

Elsevier Science B.V., Computational Materials Science  
Issue Management Physics and Materials Science  
P.O. Box 2759, 1000 CT Amsterdam  
The Netherlands  
Tel.: + 31 20 485 2517  
Fax.: + 31 20 485 2319/2431  
E-mail: h.arends@elsevier.nl



ELSEVIER

# Handbook on Semiconductors

Completely Revised and Enlarged Edition

Edited by T.S. Moss

## Volume 4: Device Physics

Volume edited by C. Hilsum

©1993 1244 pages Price: Dfl. 625.00 (US \$ 357.25)

Set price: Dfl. 1995.00 (US \$ 1140.00) ISBN 0-444-88813-6

The first edition of this volume was published 12 years ago. Since many of the devices described in it were invented 20 years or more earlier, it might have been thought that the field had reached maturity. However, the power of semiconductor physics and the ingenuity of device designers has demonstrated to the contrary. Semiconductor devices have changed so markedly in the intervening decade that this volume is effectively a new book in its own right. Less than one-third of the original material remains, and that, naturally, is largely the fundamental physics. The descriptions of devices are unique and original in each case. The basic layout of the volume is unchanged, and most of the original chapter authors have personally made many of the new advances in design and performance which they describe, as well as incorporating overviews of world progress, in both the context of traditional practice and the latest discoveries. There are two new significant changes in this new edition. The progress in the physics of panel electroluminescence no longer justifies an entire chapter. Whereas superlattices have become so significant recently that the last chapter summarises this field, reporting on the latest

advances in preparing semiconductor layers on an atomic scale. The volume includes descriptions of all today's important semiconductor devices, at a level appropriate to the physicist or engineer who is not an expert on that particular device.

**Contents:** Properties of junctions and barriers (*E.H. Roderick et al.*). Bipolar transistors and integrated circuits (*P.A.H. Hart*). MOS transistors and memories (*H.-M. Mühlhoff, D.V. McCaughan*). Charge coupled devices: physics, technology and imaging (*L.J.M. Esser, A.J.P. Theuwissen*). Microwave sources (*H.W. Thim, J. Turner*). Microwave receivers (*P.N. Robson*). Light emitting diodes (*M.H. Pilkuhn, W. Schairer*). Semiconductor lasers (*H. Kressel, D.E. Ackley*). Solar cells (*R.H. Bube*). Infrared detectors (*C.T. Elliott, N.T. Gordon*). Nuclear radiation detectors (*E.E. Haller, F.S. Goulding*). Power devices

(*Ph. Leturq, P. Rossel*). Superlattice and novel multilayer devices (*M.J. Kearney, M.J. Kelly*). Author index. Subject index.

### TO ORDER

Contact your regular supplier or:

**ELSEVIER SCIENCE B.V.**

P.O. Box 211  
1000 AE Amsterdam  
The Netherlands  
Fax: 020-5862580

Customers in the USA and  
Canada:

**ELSEVIER SCIENCE INC.**

P.O. Box 882  
Madison Square Station  
New York, NY 10159, USA  
Fax: 212-6333680

No postage will be added to prepaid book orders. Dutch Guilder price(s) quoted applies worldwide. US Dollar price(s) quoted may be subject to exchange rate fluctuations. In all other countries the Dutch guilder (Dfl.) price is definitive. Customers in The Netherlands please add 6% BTW. In New York State please add applicable sales tax. All prices are subject to change without prior notice.



## NORTH-HOLLAND

(AN IMPRINT OF ELSEVIER SCIENCE B.V.)